FEM Simulation of Generation of Bulk Acoustic Waves and Their Effects in SAW Devices

Ashish Kumar Namdeo[1], Harshal B. Nemade*[1, 2] and N. Ramakrishnan[2]
[1]Department of Electronics and Communication Engineering, [2]Centre for Nanotechnology
Indian Institute of Technology Guwahati, India
*Corresponding author: Associate Professor, Department of Electronics and Communication Engineering, Indian Institute of Technology Guwahati, India, harshal@iitg.ernet.in

Abstract: This paper presents finite element method (FEM) simulation study of the generation of bulk acoustic waves (BAWs) and their effect on the performance of surface acoustic wave (SAW) devices, using COMSOL Multiphysics™. A SAW delay line structure using *YZ*-cut lithium niobate substrate is simulated. The radiation of the bulk waves in all angles into the interior of the substrate is analyzed. The bulk acoustic waves in SAW devices can affect the device response. Since BAW reflects from the bottom surface of the substrate and interferes with the received SAW at the output, bulk radiation needs careful consideration in the design of SAW devices.

Keywords: Surface acoustic wave, SAW devices, Bulk acoustic wave (BAW), Interdigital transducer (IDT), Mass loading, COMSOL Multiphysics, FEM.

1. Introduction

The surface acoustic wave (SAW) devices have been used in electronics field as sensors, resonators, oscillators and filters etc. for almost a century [1]. Various types of transducers such as bulk acoustic wave (BAW) transducers, shear wave transducers and interdigital transducers (IDT(s)) are reported for generation and reception of acoustic waves in SAW devices. IDTs are widely used transducer in SAW devices and they are metallic comb shaped electrodes fabricated over a piezoelectric substrate. However they introduce secondary effects such as reemission, BAW, diffraction, phase speed variations, reflections and electromagnetic coupling and these effects affect the performance of the SAW device [2]. In this paper we discuss the mass loading effect of IDT electrodes in generation of BAW along the depth of the substrate.

The generation and effect of BAWs in SAW devices have been reported by following researchers. Milsom *et al*. [3] reported the radiation of BAW caused by IDT along with surface waves and distortion in the SAW device response, and they included the BAW effects in the equivalent circuit of an IDT. Honkanen *et al*. [4] studied the parasitic excitation of BAW in leaky SAW (LSAW) transducers and proposed modified coupling of mode model for LSAW transducers. Gamble *et al*. [5] performed finite element method (FEM) simulation of bulk wave generation caused by mass loading of transducers fabricated on *YZ*-cut lithium niobate substrate and reported that thick electrodes increased the electrical coupling of a uniform SAW transducer to shear vertical bulk wave. Deng [6] simulated the generation of BAW in a SAW device and discussed their possible use as a high frequency BAW device. Hashimoto *et al*. [7] theoretically investigated the effect of BAW radiation in one-port SAW resonators.

The BAW launched from IDT transforms to shear SAW and further couples with radiating BAW and significantly affecting the admittance of the device. The net amount of the radiated BAW depends on the number of finger pairs in IDT [7]. In this work we have performed FEM simulation of a SAW delay line device using COMSOL Multiphysics™ software and investigated the BAW radiation caused by the mass loading of IDT electrodes. The theory of BAW radiation in a SAW device, simulation set up, results and discussion are presented in the following sections.

2. Theory of BAW radiation in SAW devices

Theory on generation and propagation of BAW in a SAW device with IDT transducers is well explained in [2] [6]. When the IDTs are excited in a SAW device, BAW propagates inside the medium of substrate along with SAW at an angle of $\pm\alpha$ symmetric about the normal to the surface in SAW devices as shown in figure 1.

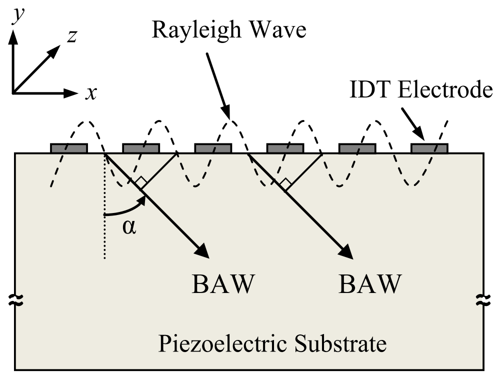

Figure 1. Schematic of BAW propagation into the substrate of a SAW device.

The constructive interference of the propagating BAW occurs for the condition given bellow [2],

$$2d\sin\alpha = \lambda_{\mathrm{B}} = V_{\mathrm{B}} / \lambda \qquad (1)$$

where, λ_{B} and V_{B} are the BAW wavelength and speed of the bulk waves, d is the thickness of the electrodes, and λ is the wavelength of SAW. If f_0 is the synchronous frequency of the SAW, then the cut off frequency of this effect can be derived from (1) as,

$$f\frac{\sin\alpha}{V_{\mathrm{B}}(\alpha)} = \frac{1}{2d} = \frac{f_0}{V_{\mathrm{R}}} \quad \Rightarrow f > \frac{V_{\mathrm{B\,min}}}{2d} \qquad (2)$$

Thus the minimal speed of the bulk wave (V_{Bmin}) is generally greater than the Rayleigh wave velocity (V_{R}). As mentioned in the previous section the generated BAWs interfere with the SAW and affect the performance of the device. The radiated BAW power from IDT highly depends on the number of IDT finger pairs and BAW radiation becomes small for IDTs with large number of finger pairs [3]. The total power P_B generated by IDT in the form of bulk wave can be expressed as integration form as

$$P_B = \int_{-s_n}^{s_n} \mathrm{Im}\left\{\Gamma(s)\,\bar{\sigma}(\omega s)\,\bar{\sigma}(\omega s)^*\right\} ds \qquad (3)$$

where, $s = 1/V_{\mathrm{B}}$ is the slowness of the bulk wave, Γ is the real function for numerical value of s, $\bar{\sigma}$ is the free charge density at the surface, ω is the radiation frequency, and $\pm s_n$ is the slowness of BAW along the x direction.

3. Simulation setup

FEM simulations of SAW devices are reported elsewhere [8], [9], [10] and [11]. The geometry, material used, boundary conditions and procedure used to perform the FEM simulation to study the generation and effects of BAW in a SAW delay line device are presented in the following paragraph. The piezoelectric module and direct solvers in COMSOL Multiphysics™ 3.5 [12] is used to perform the FEM simulation.

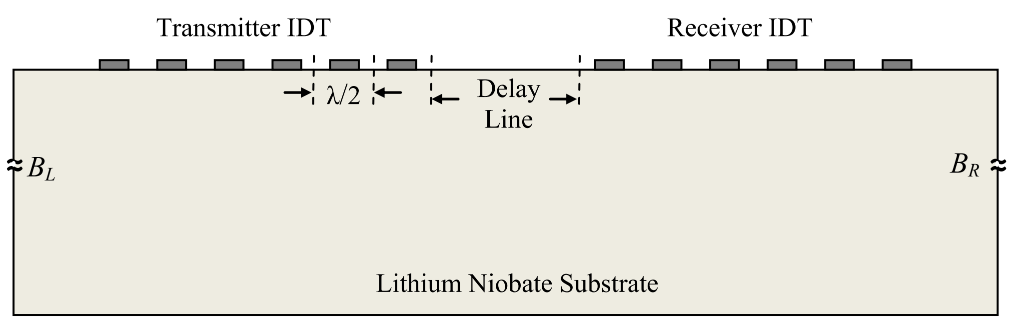

Figure 2. The 2D model of the SAW delay line device used in simulation.

A SAW delay line device with resonance frequency of 87.2 MHz is modeled as a 2D geometry as shown in the figure 2 with the following dimensions, the size of the substrate is 350 µm (8.75 λ) × 600 µm (15 λ), transmitter and receiver IDT of pitch (*p*) length 20 µm (λ/2), and delay line of length is 120 µm (3 λ). The SAW delay line device is modeled as a 2D plain strain structure. It is valid in the case of Rayleigh SAW as it has no variation and the displacement vectors have no component in *z* direction. It should be noted that the SAW energy is confined within 1 λ wavelength thickness of substrate, and the BAW travels towards the solid core of the

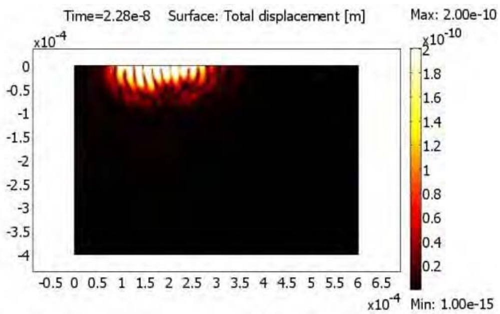

(a)

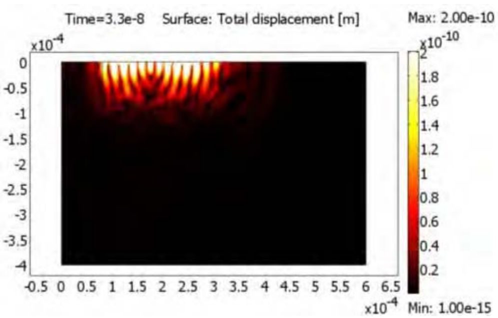

(b)

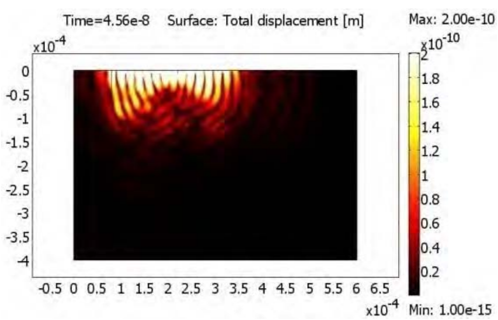

(c)

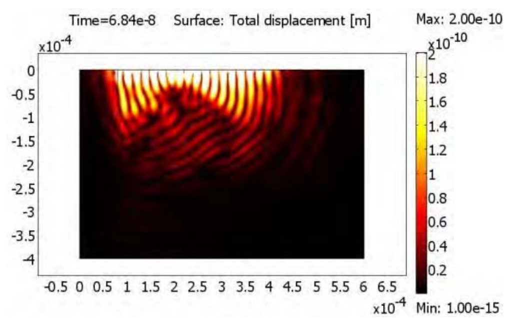

(d)

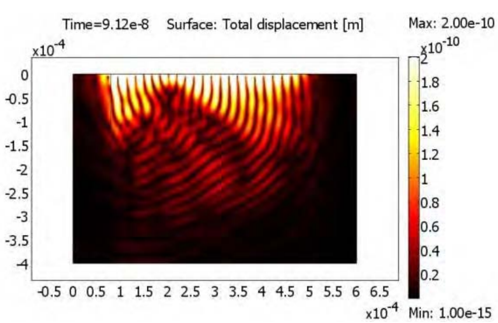

(e)

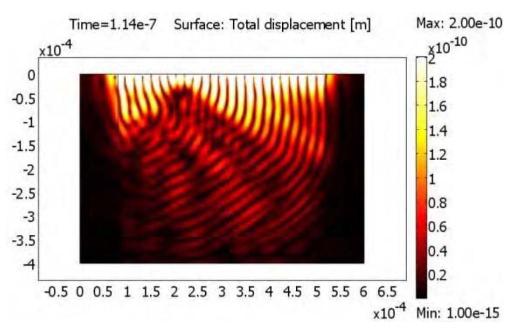

(f)

Figure 3. Surface plots of the SAW delay line device with IDT electrode thickness of 200 nm, showing propagation of BAW into the interior of the substrate observed at times (a) 22.8 ns, (b) 33.0 ns, (c) 45.6 ns, (d) 68.4 ns, (e) 91.2 ns, and (f) 114.0 ns.

substrate [2]. *YZ*-cut lithium niobate substrate is used as the substrate material in the simulation. The material properties such as dielectric constant, elastic constants, piezoelectric strain constant and density of the substrate are taken from [13]. Following boundary conditions are applied to the model. The top surface of the substrate is assumed as stress free, the bottom surface is fixed in its position, a potential of 10 V is applied for the transmitting electrodes, and critical damping is assumed to the boundaries B_R and B_L to avoid reflections at the edges of the substrate. The time domain response analysis is performed for two cases of IDT material viz., mass less electrodes, and aluminium electrode. The thickness of electrode in all cases is 200 nm. The displacement and potential of SAW at the receiver electrode, displacement of BAW at different angles are recorded during the simulation.

4. Results and discussions

The time domain analysis of the SAW delay line is performed for time duration of 114 ns. The total displacement of the substrate is recorded at different intervals of time during analysis. Figure 3 (a) to (f) show the surface plot of generation and propagation of BAW into the SAW substrate observed at time 22.8 ns, 33.0 ns, 45.6 ns, 68.4 ns, 91.2 ns, and 114.0 ns. Considering SAW velocity of 3488 m/s, time taken by the SAW to propagate from transmitter to the receiver is 34.38 ns. It can be clearly seen from the surface plots that BAW generates from IDT and travels inside the substrate. However the BAW attenuates as it travels along the depth of the medium. The values of total displacement amplitude observed at the first electrode of the receiver IDT at times 22.8 ns and 33.0 ns as extracted from figure 3 (a) and (b) are 0.124×10^{-10} m and 0.219×10^{-10} m, respectively. These values are purely BAW displacement amplitudes as they are observed before SAW reaches at the receiver IDT. Thus there is significant addition of BAW into SAW at the receiver. It is clearly evident from the surface plots shown in figure 3 (c) to (f) that, as time progresses, the BAW propagates in several angles into the interior of the substrate. The BAW radiation angles (α) calculated from figure 3 (f) are 37°, 49°, and 70°. BAW radiation after internal reflection from the substrate boundaries generates secondary waves that interfere with SAW.

We have repeated the simulation for an identical device having massless IDT electrodes. The total displacement of substrate at the end of 114 ns observed for the case of massless electrode is shown in figure 4. It can be seen that the BAW displacement is about 40 % less than the BAW displacement observed for the case of IDT with aluminium electrode of height 200 nm. Thus the mass loading of IDT increases BAW amplitude.

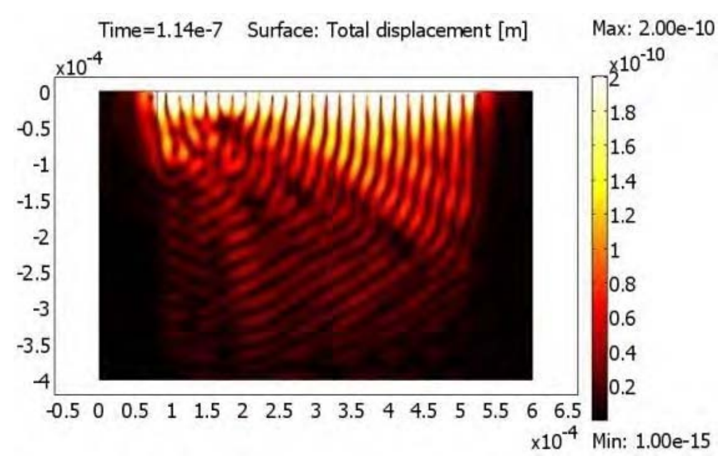

Figure 4. Surface plot of a SAW delay line device with massless IDT electrodes showing propagation of BAW into the substrate at time 114 ns.

5. Conclusions

FEM simulation of a SAW delay line is performed using COMSOL Multiphysics™. The time domain analysis shows that BAW is generated along with the SAW and it propagates into the substrate in several angles. It is also observed that BAW reaches at the receiver electrodes before SAW and interferes with SAW. The mass loading of IDT increases the intensity of BAW in a SAW device. The amplitude of BAW with aluminium IDT electrodes is about 40% more than that with massless IDT electrodes. This simulation can be further extended to study various other aspects of BAW and other secondary effects of IDT affecting the performance of SAW devices.

6. References

1. David Morgan, *Surface Acoustic Wave Filters with Applications to Electronic Communications and Signal Processing*, Elsevier Ltd., UK (2007)
2. Daniel Royer and Eugene Dieulesaint, *Elastic Waves in Solids II – Generation, Acoustic-optic Interaction, Applications*, Springer-Verlag, New York (1999)
3. Robert F. Milsom, N. H. C. Reilly, and Martin Redwood, Analysis of Generation and Detection of Surface and Bulk Acoustic Waves by Interdigital Transducers, *IEEE Transactions on Sonics and Ultrasonics*, **vol. SU-24**, no. 3, 147–164 (1977)
4. K. Honkanen, J. Koskela, V. P. Plessky, and M. M. Salomaa, Parasitic BAW Excitation in LSAW Transducers, *IEEE Ultrasonics Symposium*, 949–952 (1998)
5. Kevin J. Gamble, and Donald C. Malocha, Bulk Wave Excitation from Finite Length SAW Transducers Including Massloading, *IEEE Ultrasonics Symposium*, 77–81 (1999)
6. Mingxi Deng, Simulation of Generation of Bulk Acoustic Waves by Interdigital Transducers, *IEEE Ultrasonics Symposium*, 855–858 (2001)
7. Ken-ya Hashimoto, Masatsune Yamaguchi, Gunter Kovacs, Karl Christian Wagner, Werner Ruile, and Robert Weigel, Effects of the Bulk Wave Radiation on IDT Admittance on 42^o YX-$LiTaO_3$, *IEEE Transactions on Ultrasonics, Ferroelectrics, and Frequency Control*, **vol. 18**, no. 5, 1419–1425 (2001)
8. N. Ramakrishnan, Roy Paily Palanthikal, and Harshal B. Nemade, Mass Loading Effects of High Aspect Ratio Structures Grown over SAW Resonator, *Sensor Letters*, **vol. 8**, no. 2, 253–257 (2010)
9. M. Z. Atashbar, B. J. Bazuin, M. Simpeh, and S. Krishnamurthy, 3D FE Simulation of H_2 SAW Gas Sensor, *Sensors and Actuators B*, **vol. 111,** 213–218 (2005)
10. S. J. Ippolitto, K. Kalantar-Zadeh, D. A. Powell, and W. Wloderski, A 3-Dimensional Finite Element Approach for Simulating Acoustic Wave Propagation in Layered SAW Devices, *in proceedings IEEE Ultrasonics Symposium*, 303–306 (2003)
11. David M. Klymyshyn, Thirumalai Kannan, and Anton Kachayev, Finite Element Modeling of Electrode Mass Loading Effects in Longitudinal Leaky SAW Resonators, *Microwave and Optical Technology Letters*, **vol. 51**, no. 2 (2009)
12. COMSOL Multiphysics™ User Guide, Ver 3.2 (2005)
13. S. Ahmadi, F. Hassani, C. Korman, M. Rahaman, and M. Zaghlou, Characterization of Multi- and Single-layer Structure SAW Sensor, *Sensors 2004 in proceedings of IEEE*, **3**, 1129–1132 (2004)